Scripta Materialia 146 (2018) 5–8

Contents lists available at ScienceDirect

Scripta Materialia

journal homepage: www.elsevier.com/locate/scriptamat

Regular article

Equilibrium high entropy alloy phase stability from experiments and thermodynamic modeling

James E. Saal [a,*], Ida S. Berglund [a], Jason T. Sebastian [a], Peter K. Liaw [b], Greg B. Olson [a,c]

[a] QuesTek Innovations LLC, Evanston, IL, United States
[b] The University of Tennessee, Knoxville, TN, United States
[c] Northwestern University, Evanston, IL, United States

ARTICLE INFO

Article history:
Received 22 August 2017
Received in revised form 22 October 2017
Accepted 24 October 2017
Available online xxxx

Keywords:
CALPHAD
Phase diagram
Metal and alloys
Microstructure

ABSTRACT

Long-term stability of high entropy alloys (HEAs) is a critical consideration for the design and practical application of HEAs. It has long been assumed that many HEAs are a kinetically-stabilized metastable structure, and recent experiments have confirmed this hypothesis by observing HEA decomposition after long-term equilibration. In the present work, we demonstrate the use of the CALculation of PHAse Diagrams (CALPHAD) approach to predict HEA stability and processing parameters, comparing experimental long-term annealing observations to CALPHAD phase diagrams from a commercially-available HEA database. We find good agreement between single- and multi-phase predictions and experiments.

© 2017 Acta Materialia Inc. Published by Elsevier Ltd. All rights reserved.

High entropy alloys (HEAs) are a novel class of materials that has garnered much interest in recent years [1–10] for superior properties, including high-temperature strength, low-temperature ductility, irradiation resistance, corrosion resistance, and fatigue and fracture resistance, among many others [1,4,10–35]. As such, there is large potential for HEA components to dramatically improve performance in such critical applications as nuclear reactors, turbine engines, and automobiles.

Traditional alloy systems usually comprise a base solvent element into which a limited amount of solute elements are mixed (i.e., alloyed) into a solution, such as C into Fe and Al into Ni. HEAs are unique in that they are comprised of a disordered solid solution of multiple base elements at or near equi-atomic compositions [11–13]. The resulting high configurational entropy extends solute solubility at high heat treatment temperatures, providing extended single-phase solid solutions. The physical nature of this extended multi-component solid solution can give rise to unique properties, commonly attributed to large internal crystalline strain [4,11–16,35].

An open question in the case of HEAs is whether the solid solution established at high temperatures is a thermodynamically-stable phase at potential use temperatures. The HEA can be readily produced from casting, but there is evidence that the long-term annealing of HEAs can cause decomposition into a more traditional, multi-phase microstructure. Recent studies [36–40] have observed decomposition after long-term annealing at elevated temperatures, casting doubt on the applicability for HEA-based components during operation at such temperatures. Understanding long-term HEA stability at elevated temperatures is critical to develop HEA-based components for extreme environments.

Theoretical tools can be extremely useful for prediction of HEA phase stability, and attempts have been made at using atomistic methods, such as Molecular Dynamics (MD) and Density Functional Theory (DFT) [4,41,42]. However, such techniques are fundamentally limited by the disordered nature of the solid solution, the intricate physics for the effect of temperature, and the complexity of the phases competing with the HEA for stability. In this regard, the thermodynamic CALculation of PHAase Diagrams (CALPHAD) approach is ideally suited for predicting the long-term stability of HEAs at arbitrary temperatures. Having great success in the prediction of traditional alloy phase equilibria, the CALPHAD approach can be readily applied to HEA compositions [43–45].

The CALPHAD approach utilizes solution thermodynamic models to describe the thermodynamic properties of complex, multicomponent systems [46]. Thermodynamic and phase equilibria data are used to determine fitting parameters for the Gibbs free energies of individual phases in the system. For a solid solution phase, α, the Gibbs free energy of that phase (G^{α}) is defined by.

$$G^{\alpha} = \sum_{i}^{c} x_i G_i^{\alpha} - TS_{mix}^{ideal} + {}^{xs}G_m \quad (1)$$

where x_i is the composition of component i, G_i^{α} is the Gibbs energy of component i in the α structure, T is the temperature, S_{mix}^{ideal} is the ideal

* Corresponding author.
E-mail address: jsaal@questek.com (J.E. Saal).

https://doi.org/10.1016/j.scriptamat.2017.10.027
1359-6462/© 2017 Acta Materialia Inc. Published by Elsevier Ltd. All rights reserved.

configurational entropy (i.e., $R\sum x_i \ln x_i$, where R is the gas constant.) and $^{xs}G_m$ is the excess Gibbs energy. Databases containing these free energy descriptions can be used to predict phase equilibria and other properties for large, multicomponent alloys at arbitrary compositions by combining the functions of simpler subsystems.

For complex solid solutions (such as HEAs), the CALPHAD approach offers an accurate prediction of thermodynamic properties, such as phase stability. It is important to note that although HEAs are primarily defined by the ideal configuration entropy, the excess Gibbs energy should also be taken into account when modeling the stability of an HEA. The excess Gibbs energy ($^{xs}G_m$) encompasses the non-ideal mixing enthalpy and entropy and is typically defined in CALPHAD databases by a Redlich-Kister polynomial: [46].

$$^{xs}G_m = \sum_{i=1}^{c-1}\sum_{j>i}^{c} x_i x_j \sum_{v=0}^{n} {}^{v}L_{ij}(x_i - x_j)^v + \sum_{i=1}^{c-2}\sum_{j>i}^{c-1}\sum_{k>j}^{c} x_i x_j x_k {}^{0}L_{ijk} \quad (2)$$

where x_i is the composition of component i, $^{v}L_{ij}$ are binary interaction parameters describing the non-ideality of the binary solid solution between components i and j, v is the order of the interaction (e.g., 0 is regular, 1 is sub-regular, etc.), and $^{0}L_{ijk}$ is the regular ternary solution interaction parameter for elements i, j, and k. The temperature dependence of the L parameters defines an excess entropy contribution. The interaction parameters are fitted to experimental or theoretically-predicted thermodynamic data. For an arbitrarily large number of components, the solid-solution thermodynamics are described by summing over all of the subsystem interactions. The collection of constituent model parameters for phases described by Eqs. (1) and (2) comprise a CALPHAD database. It should be noted that the ideal configuration entropy is often cited as the stabilizing force of the HEA. However, not every equiatomic, multicomponent alloy is stable since HEA stability is dependent on both the non-ideal contributions to the excess Gibbs energy (defined by Eq. (2)) and all other competing phases.

The primary challenge in utilizing established CALPHAD techniques for the development of HEAs lies in the equiatomic nature of the HEA. CALPHAD databases are typically constructed with a focus on specific base solvent elements (e.g., Fe for steels and Ni for superalloys), which places an emphasis on achieving accuracy at corners of the composition space using binary and targeted higher-order interaction parameters. As such, specific parameters governing interactions among three or more components in face-centered-cubic (FCC) and body-centered-cubic (BCC) solid solutions are not fully populated. This trend is due to not only the application of the database to these narrow regions of composition space but also a relative lack of experimental thermochemical data for the other regions. Two CALPHAD databases specifically designed for HEAs are commercially available: TC-HEA from Thermo-Calc [47] (which includes 20 elements) and Pan-HEA from Computherm [48] (which includes 10 elements). All calculations herein will use the TC-HEA2 CALPHAD database from Thermo-Calc.

One method of visualizing the phase equilibria of a given composition is with a one-dimensional "step" diagram of the phase fraction with temperature. As shown in Fig. 1 (composition taken from Otto et al. [38]), critical features of HEA phase equilibria can be readily identified, including: the structure of the stable HEA phase [i.e., FCC, BCC, hexagonal-close-packed (HCP), etc. structures], the low-temperature phase decomposition products, and the width of the HEA single-phase region (from the solvus to the solidus). For instance, in the case of Otto et al. [38] in Fig. 1, an FCC HEA is predicted to form between 798 and 1285 °C, transforming to a Cr-rich sigma phase below 798 °C. This prediction quantitatively agrees well with Otto et al. [38], where the observed HEA is FCC and Cr-rich sigma phase particles appear to form at grain boundaries, with a solvus somewhere between 700 and 900 °C.

Beyond Otto et al. [38], several other studies [36,37,39,40] which probe the long-term stability of HEAs have been published. These are summarized in Table 1. The CALPHAD predictions for the phase equilibria at the heat-treatment temperature, solvus, equilibrium solidus, and Scheil solidus (described later) are also given. Essentially, fairly good qualitative agreement is found, with the CALPHAD database correctly predicting the HEA structure and the appearance of secondary phases at the experimental heat-treatment temperatures.

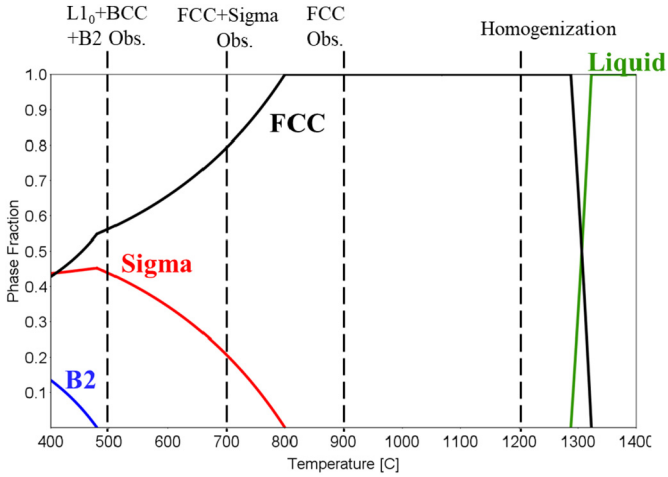

Fig. 1. CALPHAD-predicted temperature vs. phase fraction phase diagram for the CoCrFeMnNi HEA, including the homogenization temperature and experimental phase observations of Otto et al. [38] From the CALPHAD predictions, the sigma phase is Cr-, Fe-, and Mn-rich and the B2 is Co- and Fe-rich.

Many of the compositions summarized in Table 1 lie along a linear addition of Al, namely $Al_xCoCrFeNi$. The CALPHAD approach can be used to take a step diagram, as in Fig. 1, and extend it across compositions, to form a two-dimensional composition-temperature phase diagram. For $Al_xCoCrFeNi$, the predicted phase diagram for $x < 0 < 1$ is shown in Fig. 2. There is qualitative agreement between the results of Tang et al. [40] and the CALPHAD prediction. Tang et al. [40] observed a single-phase FCC structure at 1250 °C from $x = 0.3$ and $x = 0.5$, forming a BCC/B2 second phase at $x = 0.7$. The CALPHAD phase diagram predicts a single-phase field (FCC) below $x = 0.42$ and a two-phase (FCC + BCC) field above $x = 0.42$. The difference in phase-boundary compositions can be explained by the inaccuracy of the CALPHAD database thermodynamic parameters, as discussed earlier, and/or an inadequate heat treatment to achieve equilibrium microstructures.

An assumption of the above calculations is that the HEA microstructure is homogeneous. In reality, the as-cast microstructure likely consists of dendritic inhomogeneity, caused by the partitioning of slow diffusing/high-melting point elements from fast diffusing/low-melting point elements. Such inhomogeneities introduce variation in not only the composition but also the solidus (incipient melting) temperature. The CALPHAD approach is capable of predicting the compositional evolution of a dendrite during solidification by coupling databases of thermodynamic parameters and diffusional kinetic parameters. Although a common tactic in Ni- and Fe-based alloy modeling, CALPHAD kinetic databases are not readily available for HEAs.

A thermodynamic approximation to the kinetic solidification simulation is possible with the Scheil simulation approach [49], in which diffusivities in the liquid and solid are assumed to be infinite and zero, respectively. The results of such a Scheil simulation for the HEA of Otto et al. [38] predict a solidus (1154 °C) lower than the equilibrium solidus in Fig. 1 (1285 °C) because the composition of the melt is allowed to evolve. This Scheil solidus serves as an effective lower limit to the solidus for a given system and can be used as a safe upper limit for the choice of homogenization temperature to avoid incipient melting of the edge of the dendrite. Further, the Scheil simulation also makes predictions as to phase equilibria during solidification, indicating the likely precipitation of secondary phases in the interdendritic region of the as-cast microstructure. The systems of Tang et al. [40] and Jones et

Table 1
Table summarizing experimental data and CALPHAD predictions for long-term annealed HEAs, including: composition, homogenization temperature and time, aging temperature and time, observed phases, and CALPHAD predictions (equilibrium phases at the aging temperature, solvus temperature, equilibrium solidus temperature, and Scheil solidus temperature). Note that reports of multiple FCC structures for a single nominal composition indicate observations of separate FCC phases of unique compositions.

	Composition	Homog conditions	Aging conditions	Observed phases	CALPHAD phases	Solvus [°C]	Equil. solidus [°C]	Scheil solidus [C°]
Otto et al. [38]	CoCrFeMnNi	1200 °C 48 h	500 °C 12,000 h	$L1_0$, BCC, B2	FCC, Sigma	798	1285	1154
	CoCrFeMnNi	1200 °C 48 h	700 °C 12,000 h	FCC, Sigma	FCC, Sigma	798	1285	1154
	CoCrFeMnNi	1200 °C 48 h	900 °C 12,000 h	FCC	FCC	798	1285	1154
Pickering et al. [39]	CoCrFeMnNi	1240 °C 100 h	700 °C 1000 h	FCC, Sigma, $M_{23}C_6$	FCC, Sigma	798	1285	1154
He et al. [36]	CoCrFeNi	None	750 °C 800 h	FCC, FCC	FCC	677	1445	1427
	$Al_{0.1}$CoCrFeNi	None	750 °C 800 h	FCC, FCC, ?Cr-rich	FCC, B2	777	1426	1378
Tang et al. [40]	$Al_{0.3}$CoCrFeNi	1250 °C 50 h	1250 °C 1000 h	FCC	FCC	1097	1387	1312
	$Al_{0.5}$CoCrFeNi	1250 °C 50 h	1250 °C 1000 h	FCC	FCC, B2	1333	1333	1314
	$Al_{0.7}$CoCrFeNi	1250 °C 50 h	1250 °C 1000 h	FCC, BCC/B2	FCC, B2, BCC	1337	1337	1320
Jones et al. [37]	$Al_{0.5}$CoCrCuFeNi	None	1000 °C 1000 h	FCC, FCC, $L1_2$	FCC, Liquid, B2	1270	990	914

al. [37] may be particularly susceptible to second-phase precipitation upon solidification. The collection of these phase equilibria and Scheil predictions can be used to estimate the ease of achieving a homogenous, clean HEA microstructure after casting. In essence, minimizing both the temperature range of solidification (from initial to final solidification) and the temperature range within which secondary solid phases are present should yield homogeneous as-cast microstructures.

Further, the reports of He et al. [36] and Jones et al. [37] regarding phase equilibria in the Al_xCoCrFeNi phase diagram in Fig. 2 observe second phases at compositions at $x \leq 0.5$, qualitatively disagreeing with Tang et al. [40]. This trend can likely be attributed to the lack of a homogenization treatment in their measurement. Indeed, the phases that He et al. [36] and Jones et al. [37] observe are FCC's with different compositions, which would be expected in an inhomogeneous dendritic microstructure. Scheil simulations can also predict the degree of segregation during solidification, describing the composition of the solid across a dendrite, from the core to the edge. The segregation can thus be quantified by the ratio of the edge composition to the core. For example, segregation ratios[1] for the $Al_{0.5}$CoCrCuFeNi HEA of Jones et al. [37] suggest a core rich in Co/Cr/Fe and an edge rich in Al/Cu/Ni. This trend agrees very well with Jones et al. [37] observations of a dendritic microstructure in the as-cast alloy comprising a Co/Cr/Fe-rich FCC dendrite and an Al/Cu-rich interdendritic FCC phase.

In summary, the CALPHAD approach and commercial thermodynamic databases can be used to accurately predict phase equilibria in HEA systems when compared to observations for systems undergoing long-term heat treatments. By comparing CALPHAD predictions to experimental references, we demonstrated that a proper post-cast homogenization is critical to eliminate the appearance of metastable inhomogeneity, which has been previously reported as multiple FCC phases after aging. Scheil simulations can be used to assess the need for homogenization by predicting the degree of segregation during solidification. Lastly, there is a need for data on proper HEA phase equilibria to improve the quantitative accuracy of CALPHAD databases. Accurate thermodynamic and kinetic CALPHAD databases form the foundation of materials design, and realizing the full potential of HEAs requires such computational tools to optimize alloy parameters within the complexity of the HEA composition space.

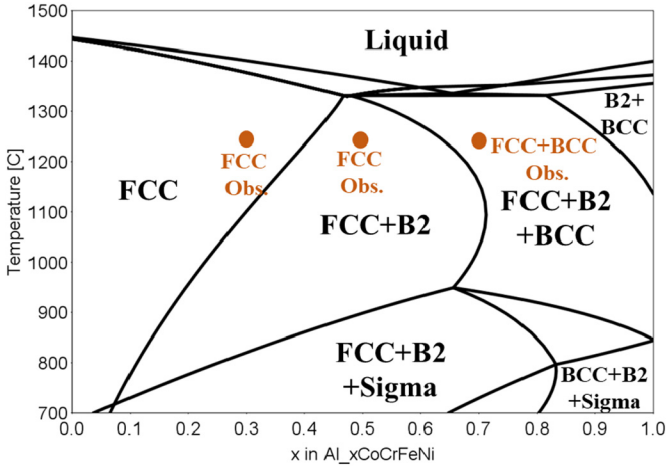

Fig. 2. CALPHAD-predicted Al_xCoCrFeNi temperature vs. composition phase diagram, including the experimental observations of the homogenized HEAs from Tang et al. [40].

Acknowledgement

We gratefully acknowledge the funding of the Department of Energy Office of Science and the Small Business Innovation Research program (contract number DE-SC0013220).

References

[1] Z. Li, K.G. Pradeep, Y. Deng, D. Raabe, C.C. Tasan, Nature 534 (2016) 227–230.
[2] O.N. Senkov, J.D. Miller, D.B. Miracle, C. Woodward, Nat. Commun. 6 (2015) 6529.
[3] Y.H. Jo, S. Jung, W.M. Choi, S.S. Sohn, H.S. Kim, B.J. Lee, N.J. Kim, S. Lee, Nat. Commun. 8 (2017) 15719.
[4] L.J. Santodonato, Y. Zhang, M. Feygenson, C.M. Parish, M.C. Gao, R.J.K. Weber, J.C. Neuefeind, Z. Tang, P.K. Liaw, Nat. Commun. 6 (2015) 5964.
[5] C.L. Tracy, S. Park, D.R. Rittman, S.J. Zinkle, H. Bei, M. Lang, R.C. Ewing, W.L. Mao, Nat. Commun. 8 (2017) 15634.
[6] Y. Zhang, G.M. Stocks, K. Jin, C. Lu, H. Bei, B.C. Sales, L. Wang, L.K. Béland, R.E. Stoller, G.D. Samolyuk, M. Caro, A. Caro, W.J. Weber, Nat. Commun. 6 (2015) 8736.
[7] Z. Zhang, M.M. Mao, J. Wang, B. Gludovatz, Z. Zhang, S.X. Mao, E.P. George, Q. Yu, R.O. Ritchie, Nat. Commun. 6 (2015) 10143.

[1] Al = 3.0, Co = 0.003, Cr = 0.04, Cu = 31.8, Fe = 0.09, Ni = 1.9.

[8] F. Zhang, Y. Wu, H. Lou, Z. Zeng, V.B. Prakapenka, E. Greenberg, Y. Ren, J. Yan, J.S. Okasinski, X. Liu, Y. Liu, Q. Zeng, Z. Lu, Nat. Commun. 8 (2017) 15687.
[9] Y. Zou, H. Ma, R. Spolenak, Nat. Commun. 6 (2015) 7748.
[10] B. Gludovatz, A. Hohenwarter, D. Catoor, E.H. Chang, E.P. George, R.O. Ritchie, Science 345 (2014) 1153–1158 (80-.).
[11] B. Cantor, I.T.H. Chang, P. Knight, A.J.B. Vincent, Mater. Sci. Eng. A 375–377 (2004) 213–218.
[12] J.-W. Yeh, S.-K. Chen, S.-J. Lin, J.-Y. Gan, T.-S. Chin, T.-T. Shun, C.-H. Tsau, S.-Y. Chang, Adv. Eng. Mater. 6 (2004) 299–303.
[13] Y. Zhang, T.T. Zuo, Z. Tang, M.C. Gao, K.A. Dahmen, P.K. Liaw, Z.P. Lu, Prog. Mater. Sci. 61 (2014) 1–93.
[14] M.-H. Chuang, M.-H. Tsai, W.-R. Wang, S.-J. Lin, J.-W. Yeh, Acta Mater. 59 (2011) 6308–6317.
[15] Y. Shi, B. Yang, P.K. Liaw, Metals (Basel, Switz.) 7 (2017) 43.
[16] Z. Tang, L. Huang, W. He, P. Liaw, Entropy 16 (2014) 895–911.
[17] B.-R. Chen, A.-C. Yeh, J.-W. Yeh, Sci Rep 6 (2016) 22306.
[18] T.K. Chen, T.T. Shun, J.W. Yeh, M.S. Wong, Surf. Coat. Technol. 188–189 (2004) 193–200.
[19] D.B. Miracle, O.N. Senkov, Acta Mater. 122 (2017) 448–511.
[20] J.-W. Yeh, Ann. Chim. Sci. Mater. 31 (2006) 633–648.
[21] C.-J. Tong, M.-R. Chen, J.-W. Yeh, S.-J. Lin, S.-K. Chen, T.-T. Shun, S.-Y. Chang, Metall. Mater. Trans. A 36 (2005) 1263–1271.
[22] J.-W. Yeh, S.-J. Lin, T.-S. Chin, J.-Y. Gan, S.-K. Chen, T.-T. Shun, C.-H. Tsau, S.-Y. Chou, Metall. Mater. Trans. A 35 (2004) 2533–2536.
[23] Y. Zhang, Y.J. Zhou, J.P. Lin, G.L. Chen, P.K. Liaw, Adv. Eng. Mater. 10 (2008) 534–538.
[24] O.N. Senkov, G.B. Wilks, D.B. Miracle, C.P. Chuang, P.K. Liaw, Intermetallics 18 (2010) 1758–1765.
[25] S. Singh, N. Wanderka, B.S. Murty, U. Glatzel, J. Banhart, Acta Mater. 59 (2011) 182–190.
[26] M.A. Hemphill, T. Yuan, G.Y. Wang, J.W. Yeh, C.W. Tsai, A. Chuang, P.K. Liaw, Acta Mater. 60 (2012) 5723–5734.
[27] M. Seifi, D. Li, Z. Yong, P.K. Liaw, J.J. Lewandowski, JOM 67 (2015) 2288–2295.
[28] Z. Tang, T. Yuan, C.-W. Tsai, J.-W. Yeh, C.D. Lundin, P.K. Liaw, Acta Mater. 99 (2015) 247–258.
[29] C.-Y. Hsu, C.-C. Juan, S.-T. Chen, T.-S. Sheu, J.-W. Yeh, S.-K. Chen, JOM 65 (2013) 1829–1839.
[30] C.-Y. Hsu, J.-W. Yeh, S.-K. Chen, T.-T. Shun, Metall. Mater. Trans. A 35 (2004) 1465–1469.
[31] H. Diao, X. Xie, F. Sun, K.A. Dahmen, P.K. Liaw, High-entropy Alloy, Springer International Publishing, Cham, 2016 181–236.
[32] J.M. Zhu, H.M. Fu, H.F. Zhang, A.M. Wang, H. Li, Z.Q. Hu, J. Alloys Compd. 509 (2011) 3476–3480.
[33] Y.J. Zhou, Y. Zhang, Y.L. Wang, G.L. Chen, Appl. Phys. Lett. 90 (2007) 181904.
[34] Y.Y. Chen, T. Duval, U.D. Hung, J.W. Yeh, H.C. Shih, Corros. Sci. 47 (2005) 2257–2279.
[35] M.C. Gao, J.-W. Yeh, P.K. Liaw, Y. Zhang, High-Entropy Alloys: Fundamentals and Applications, Springer, 2016.
[36] F. He, Z. Wang, Q. Wu, J. Li, J. Wang, C.T. Liu, Scr. Mater. 126 (2017) 15–19.
[37] N.G. Jones, J.W. Aveson, A. Bhowmik, B.D. Conduit, H.J. Stone, Intermetallics 54 (2014) 148–153.
[38] F. Otto, A. Dlouhý, K.G. Pradeep, M. Kuběnová, D. Raabe, G. Eggeler, E.P. George, Acta Mater. 112 (2016) 40–52.
[39] E.J. Pickering, R. Muñoz-Moreno, H.J. Stone, N.G. Jones, Scr. Mater. 113 (2016) 106–109.
[40] Z. Tang, O.N. Senkov, J.D. Poplawsky, C. Zhang, F. Zhang, C.D. Lundin, P.K. Liaw, Under Prep, 2017.
[41] Z. Leong, J.S. Wróbel, S.L. Dudarev, R. Goodall, I. Todd, D. Nguyen-Manh, Sci Rep 7 (2017) 39803.
[42] A. Sharma, P. Singh, D.D. Johnson, P.K. Liaw, G. Balasubramanian, Sci Rep 6 (2016) 31028.
[43] S.-M. Liang, R. Schmid-Fetzer, J. Phase Equilib. Diffus. 38 (2017) 369–381.
[44] R. Feng, M. Gao, C. Lee, M. Mathes, T. Zuo, S. Chen, J. Hawk, Y. Zhang, P. Liaw, Entropy 18 (2016) 333.
[45] C. Zhang, F. Zhang, H. Diao, M.C. Gao, Z. Tang, J.D. Poplawsky, P.K. Liaw, Mater. Des. 109 (2016) 425–433.
[46] H.L. Lukas, S.G. Fries, B. Sundman, Computational Thermodynamics: The CALPHAD Method, Cambridge University Press, 2007.
[47] Available at: http://www.thermocalc.com/products-services/databases/thermodynamic/, Accessed date: 6 July 2017.
[48] Available at: http://www.computherm.com/index.php?route=product/category&path=59_83, Accessed date: 6 July 2017.
[49] O. Senkov, F. Zhang, J. Miller, Entropy 15 (2013) 3796–3809.